PAPER • **OPEN ACCESS**

Development of Lateral Prestress in High-Strength Concrete-Filled FRP Tubes

To cite this article: T Vincent and T Ozbakkaloglu 2018 *IOP Conf. Ser.: Mater. Sci. Eng.* **307** 012062

View the article online for updates and enhancements.

IOP ebooks™

Bringing you innovative digital publishing with leading voices to create your essential collection of books in STEM research.

Start exploring the collection - download the first chapter of every title for free.

This content was downloaded from IP address 129.96.87.58 on 18/10/2018 at 23:28

IOP Conf. Series: Materials Science and Engineering **307** (2018) 012062 doi:10.1088/1757-899X/307/1/012062

Development of Lateral Prestress in High-Strength Concrete-Filled FRP Tubes

T Vincent[1] and T Ozbakkaloglu[2]

[1] College of Science and Engineering, Flinders University, Adelaide, South Australia, Australia 5042
[2] School of Civil, Environmental and Mining Engineering, The University of Adelaide, Adelaide, South Australia, Australia 5005

E-mail: thomas.vincent@flinders.edu.au

Abstract. This paper reports on an experimental investigation into the axial and lateral strain development of fiber reinforced polymer (FRP) confined high-strength concrete (HSC) with prestressed FRP shells. A total of 24 aramid FRP (AFRP)-confined concrete specimens were manufactured as concrete-filled FRP tubes (CFFTs) with instrumentation to measure the strain variations during application of prestress, removal of end constraints and progressive prestress losses. Prestressed CFFT specimens were prepared with three different dose rates of expansive mineral admixture to create a range of lateral prestress applied to AFRP tubes manufactured with sheet thicknesses of 0.2 or 0.3 mm/ply and referred to as lightly- or well-confined, respectively. In addition to these three levels of prestress, non-prestressed companion specimens were manufactured and tested to determine baseline performance. The experimental results from this study indicate that lateral prestressing of CFFTs manufactured with HSC can be achieved by varying the expansive mineral admixture dose rate with a lateral prestress of up to 7.3 MPa recorded in this study. Significant strain variations were measured during removal of the end constraints with up to 700 microstrain recorded in the axial direction. Finally, the measurement of prestress losses for the month following prestress application revealed minimal progressive losses, with only 250 and 100 με recorded for the axial and hoop strains, respectively.

1. Introduction

The use of fiber reinforced polymer (FRP) composites as a wrap or jacket for the confinement of concrete columns has gained significant research attention over the last two decades. Recent reviews [1-5] have revealed that many studies have examined both FRP-wrapped concrete (e.g., [6-9]), intended for strengthening existing concrete columns and concrete-filled FRP tubes (CFFTs) (e.g., [10-24]), intended for construction of new columns, which has resulted in a large number of proposed models (e.g., [25-30]).

Recently the construction industry has experienced a progressive increase in the use of higher strength concretes (HSCs) over normal strength concrete (NSC) due to the improved performance and reduced dead loads offered. However, as was recently demonstrated in Vincent and Ozbakkaloglu [31], FRP-confined HSC columns have a tendency to experience a more rapid and uncontrolled expansion during activation of the confinement mechanism compared to the more progressive expansion of NSC

Content from this work may be used under the terms of the Creative Commons Attribution 3.0 licence. Any further distribution of this work must maintain attribution to the author(s) and the title of the work, journal citation and DOI.
Published under licence by IOP Publishing Ltd

due to the higher brittleness of HSC [3, 14]. The addition of prestrain to the FRP fibers is a potential technique to overcome the uncontrolled expansion, however limited studies exist on the application of prestress to FRP confined concrete.

To address this research gap, this paper reports on an experimental program to monitor prestress development for FRP-confined HSC specimens manufactured with four different dose rates of expansive mineral admixture. Variations in axial and lateral strains in the FRP shell are reported for the 3 key prestress stages: application of prestress; removal of end constraints; and progressive prestress losses. Initially, the details of the test program are presented followed by a comparison of the axial and hoop strain development during these 3 key stages. Finally, discussions on the effects of the key parameters are provided.

2. Test Database

2.1. Details of manufactured specimens

A total of 24 test specimens were manufactured and laboratory tested for this experimental program. All specimens were manufactured as cylindrical aramid FRP (AFRP)-confined concrete specimens with a diameter of 152 mm and height of 305 mm. Four different concrete mixes were used in the experimental program with average compressive strengths (f'_{co}) of 100.2 and 110.3 MPa for the expansive and non-expansive mixes, respectively. The FRP tubes for all specimens were constructed using a manual wet layup technique from a single continuous sheet to create four layers. The tubes were allowed 24 hours to cure before concrete was cast inside to create concrete-filled FRP tubes (CFFTs). Nominal fiber thicknesses of either 0.2 or 0.3 mm/layer were used to manufacture specimens with a total fiber thickness (t_f) of either 0.8 or 1.2 mm, referred to as lightly- or well-confined, respectively. Table 1 provides a summary of the test specimens.

Table 1. Test specimen details

Total fiber thickness, t_f (mm)	Concrete Mix	Concrete strength, f'_{co} (MPa)	f_{lu}/f'_{co}	Number of specimens
0.8	Mix 1	110.3	0.25	3
	Mix 2	100.2	0.27	3
	Mix 3	100.2	0.27	3
	Mix 4	100.2	0.27	3
1.2	Mix 1	110.3	0.37	3
	Mix 2	100.2	0.41	3
	Mix 3	100.2	0.41	3
	Mix 4	100.2	0.41	3

To laterally prestrain the fibers in the AFRP shell, the CFFT specimens were placed in steel prestressing rigs which consisted of 16-mm thick steel end caps connected by 16-mm diameter threaded rod. The specimens were placed in these rigs immediately after casting of concrete into the FRP tubes to restrain the extension of the concrete in the axial direction and limit the expansion to the lateral direction. For consistency, control specimens from all four concrete mixes were cast in steel tubes to replicate curing conditions experienced in the FRP tubes. This configuration also limited the tendency for loss of integrity for the expansive concrete mixes as they cured. These steel tubes were carefully cut and removed from the control cylinders immediately prior to testing f'_{co}. An example of the prestressing rigs can be seen in Figure 1.

a) *b)*

Figure 1. Steel end caps and threaded rod used to create the prestressing rig: a) steel tube specimen prior to casting of control specimen; b) CFFT specimen during concrete curing

To determine dose rates of expansive admixture numerous trial mixes were prepared to target fiber prestrain levels at 0, 10, 20 and 30% of their ultimate tensile strain (ε_f) for the lightly-confined specimens. Final mix designs and material properties of the fiber and FRP composite are provided in Tables 2 and 3 respectively, with a more detailed explanation of the experimental program provided elsewhere [32].

Table 2. Concrete mix proportions

Concrete constituent	Mix 1	Mix 2	Mix 3	Mix 4
Cement (kg/m^3)	462	462	462	462
Silica fume (kg/m^3)	88	88	88	88
Sand (kg/m^3)	700	647	629	618
Coarse Aggregate (kg/m^3)	1049	970	942	927
Water (kg/m^3)	136	163	166	172
Superplasticiser (kg/m^3)	15	14	14	13
Expansive admixture (kg/m^3)	0	105	143	165
Water to binder ratio*	0.269	0.266	0.255	0.255

** Binder content includes cement, silica fume and expansive admixture*

Table 3. Fiber and FRP composite material properties

Type	Nominal thickness t_f (mm/ply)	Material properties					
		From manufacturer			Determined by coupon tests		
		Ultimate Tensile stress f_f (MPa)	Ultimate Tensile strain ε_f (%)	Elastic modulus E_f (GPa)	Ultimate tensile stress f (MPa)	Ultimate tensile strain ε (%)	Elastic modulus E (GPa)
Aramid fiber	0.2 or 0.3	2600	2.20	118.2	2390*	1.86	128.5*

** Values determined by using nominal thickness of fibers*

2.2. Instrumentation

Each of the 24 test specimens was instrumented with two 5-mm unidirectional strain gauges attached to the external FRP tube surface at specimen mid-height. These strain gauges were aligned horizontally on opposing sides of the AFRP shell outside the overlap region to measure hoop strain development. These strain gauges recorded the prestrain development in the FRP tubes for over 50 days as the concrete cured, with measurements commencing immediately after casting of the concrete.

To monitor the influence of end constraints removal on prestress loss, the six specimens with the highest dose rate of expansive admixture were instrumented to measure axial and hoop strain development during this stage. These specimens were allocated two additional 5-mm strain gauges located at mid-height on opposing sides of the FRP tube mounted in the axial direction.

A single specimen was instrumented to monitor the amount of progressive prestress relaxation over a four week period after removal of the prestressing rig. This specimen had four 5-mm strain gauges attached to the surface of the FRP tube to monitor axial strain development and an additional four 5-mm gauges to monitor lateral strain development. These strain gauges were located at specimen mid-height outside the overlap region and were mounted with equal spacing around specimen perimeter.

3. Test Results

3.1. Lateral prestrain development

Lateral prestress development due to expansion of the curing concrete was recorded for over 50 days. Figure 2 presents the average lateral prestrain development and corresponding lateral prestress for the four concrete mixes presented in Table 2.

Figure 2(a) presents the lateral prestrain development for the lightly-confined test specimens, where it can be seen that a prestrain of approximately 4000 to 7000 με developed. Figure 2(b) presents a similar strain development trend for the well-confined test specimens with a prestrain of approximately 3000 to 5000 με recorded. It can be seen in these figures that, similar to concrete compressive strength development, the majority of the lateral prestress was observed to develop within 28 days from concrete casting. It is also evident in this comparison that as expected, higher lateral strains developed in the lightly-confined specimens compared to their well-confined counterparts and an increase in lateral strain development resulted from an increase in expansive mineral admixture dose rate. A closer inspection of these figures reveals that both series of specimens without expansive admixtures exhibited a slight compressive strain of approximately 50 με. This outcome can be attributed to a slight amount of concrete shrinkage overcoming the initial tensile strains caused by the hydrostatic pressure of the fresh concrete mix.

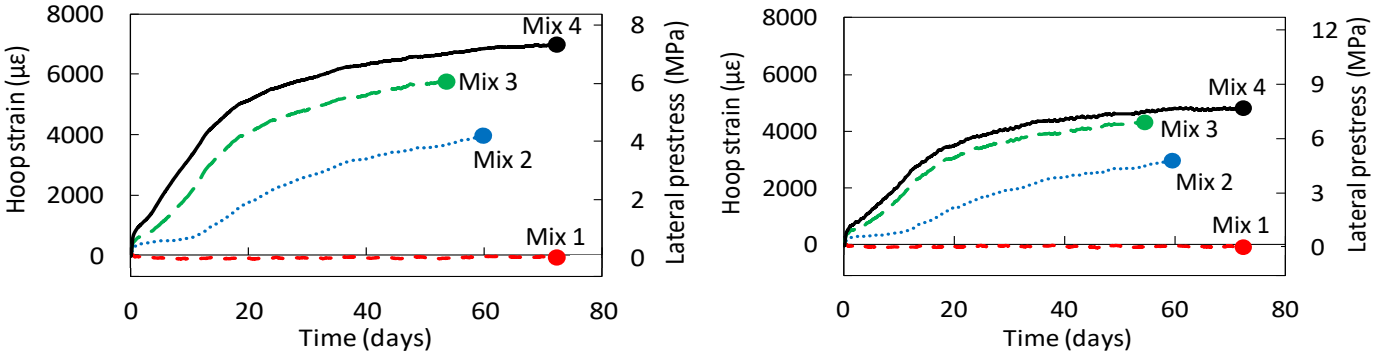

Figure 2. Hoop strain and corresponding lateral prestress development in the FRP tube: a) specimens with t_f = 0.8 mm; b) specimens with t_f = 1.2 mm.

3.2. Removal of end constraints

As shown in Figure 3, removal of the prestressing rig lead to the specimens experiencing a reduction in the tensile hoop strain of up to 60 με. In addition to this, up to 700 με tensile strain in the axial direction was developed due to the concrete expansion as the constraints were released. This outcome indicates that axial strains were significantly more influenced by removal of end constraints compared to variations in lateral prestress. It also indicates that tensile strain variations were sufficient for the internal concrete to experience tensile cracks. It is worth noting that in practice these axial tensile strains are expected to be overcome by the axial loads present in the column during construction.

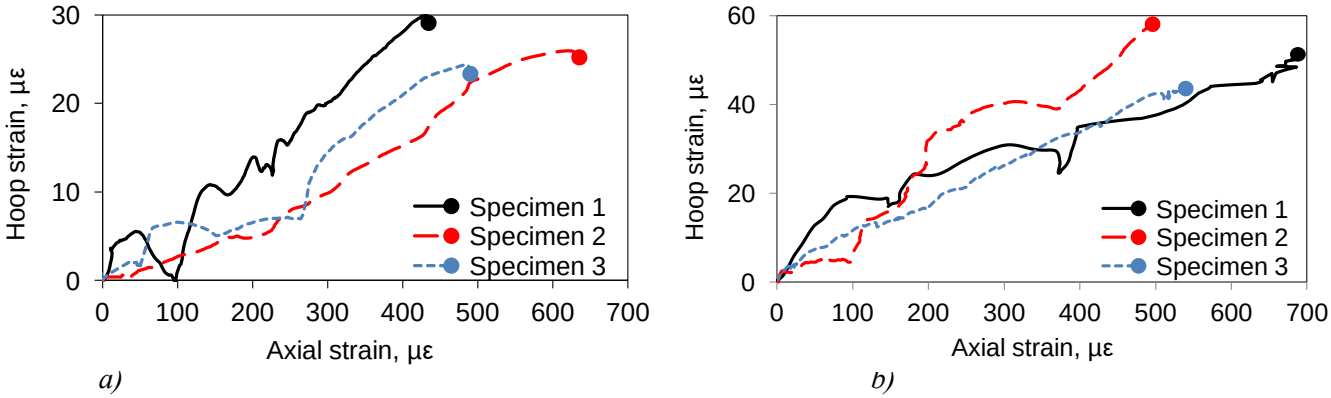

Figure 3. Hoop strain variations during removal of specimens from steel end constraints: a) specimens with t_f = 0.8 mm; b) specimens with t_f = 1.2 mm.

3.3. Prestress losses

In addition to the prestress development and recorded prestrain reductions, further time dependent prestress losses were examined on a single well confined specimen with the highest level of prestress from Mix 4. Figures 4(a) and 4(b) present the average development of the prestress losses in the axial and hoop directly, respectively. This outcome indicates minimal progressive prestrain losses with only approximately 250 and 100 με recorded over a month for the axial and hoop strains, respectively.

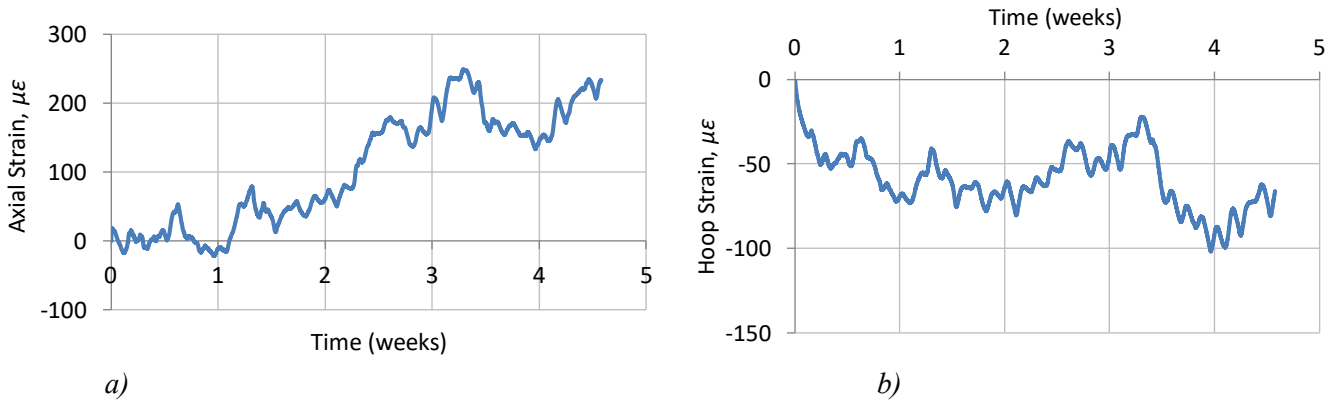

Figure 4. Time dependent variations in prestress losses after removal of end constraints: a) axial strain losses; b) hoop strain losses.

4. Conclusions

This paper has reported the results of an investigation into the axial and lateral strain development of FRP confined high-strength concrete with prestressed FRP shells and the following conclusions are presented:

1. Development of lateral prestress in CFFTs manufactured with HSC is achievable by adding expansive mineral admixture to the concrete mix. Similar to concrete compressive strength development, the majority of the lateral prestress was observed to develop within 28 days from concrete casting.
2. The amount of lateral prestress in the FRP fibers can be controlled by varying the expansive mineral admixture dose rate in the concrete mix design. A dose rate of up to 30% addition to

the total cementitious content resulted in a lateral prestress of up to 7.3 MPa for lightly-confined specimens.

3. Removal of end constraints for prestressed CFFTs has only a minor effect on the amount of prestress developed in the specimen. However, this procedure influences the axial strains significantly and the tensile strains recorded are sufficient to cause tensile cracks in the internal concrete.
4. CFFT columns with prestressed fibers experience minimal progressive prestrain losses within the first four weeks following prestress application.

References

[1] Ozbakkaloglu, T., J.C. Lim, and T. Vincent, 2013 FRP-confined concrete in circular sections: Review and assessment of the stress-strain models. *Eng. Struct.* **49**: p. 1068-1088.
[2] Ozbakkaloglu, T. and J.C. Lim, 2013 Axial compressive behavior of FRP-confined concrete: Experimental test database and a new design-oriented model. *Compos. Part B.* **55**: p. 607 - 634.
[3] Lim, J.C. and T. Ozbakkaloglu, 2014 Confinement model for FRP-confined high-strength concrete. *ASCE, J. Compos. Constr.* **18**(4): p. 04013058.
[4] Lim, J.C. and T. Ozbakkaloglu, 2014 Design model for FRP-confined normal- and high-strength concrete square and rectangular columns. *Mag. Conc. Res.* **66**(20): p. 1020-1035.
[5] Ozbakkaloglu, T., 2013 Compressive behavior of concrete-filled FRP tube columns: Assessment of critical column parameters. *Eng. Struct.* **51**: p. 151-161.
[6] Ilki, A., et al., 2008 FRP Retrofit of Low and Medium Strength Circular and Rectangular Reinforced Concrete Columns. *ASCE J. Mater. Civ. Eng.* **20**(2): p. 169 - 188.
[7] Rousakis, T. and A. Karabinis, 2008 Substandard reinforced concrete members subjected to compression: FRP confining effects. *Mater. Struct.* **41**(9): p. 1595 - 1611.
[8] Wang, Z., et al., 2012 CFRP-confined square RC columns. I: Experimental investigation. *ASCE, J. Compos. Constr.* **16**(2): p. 150 - 160.
[9] Ozbakkaloglu, T. and E. Akin, 2012 Behavior of FRP-confined normal- and high-strength concrete under cyclic axial compression. *ASCE, J. Compos. Constr.* **16**(4): p. 451-463.
[10] Xie, T. and T. Ozbakkaloglu, 2015 Behavior of Steel Fiber-Reinforced High-Strength Concrete-Filled FRP Tube Columns under Axial Compression. *Engineering Structures*. **90**: p. 158-171.
[11] Ozbakkaloglu, T. and T. Xie, 2016 Geopolymer Concrete-Filled FRP Tubes: Behavior of Circular and Square Columns under Axial Compression. *Compos. Part B.* **96**: p. 215-230.
[12] Xie, T. and T. Ozbakkaloglu, 2016 Behavior of Recycled Aggregate Concrete-Filled Basalt and Carbon FRP Tubes. *Constr. Build. Mater.* **105**: p. 132-143.
[13] Fam, A. and S. Rizkalla, 2001 Behavior of axially loaded concrete-filled circular fiber-reinforced polymer tubes. *ACI Struct. J.* **98**(3).
[14] Ozbakkaloglu, T. and T. Vincent, 2014 Axial compressive behavior of circular high-strength concrete-filled FRP tubes. *ASCE, J. Compos. Constr.* **18**(2): p. 04013037.
[15] Vincent, T. and T. Ozbakkaloglu, 2014 Influence of slenderness on stress-strain behavior of concrete-filled FRP tubes: an experimental study. *ASCE, J. Compos. Constr.* **19**(1): p. 04014029.
[16] Lim, J.C. and T. Ozbakkaloglu, 2015 Influence of Concrete Age on Stress-Strain Behavior of FRP-Confined Normal- and High-Strength Concrete. *Constr. Build. Mater.* **82**: p. 61-70.
[17] Vincent, T. and T. Ozbakkaloglu, 2016 Influence of overlap configuration on compressive behavior of CFRP-confined normal- and high-strength concrete. *Mater. Struct.* **49**(4): p. 1245-1268.
[18] Ozbakkaloglu, T., 2013 Axial compressive behavior of square and rectangular high-strength concrete-filled FRP tubes. *ASCE, J. Compos. Constr.* **17**(1): p. 151-161.
[19] Ozbakkaloglu, T. and Y. Idris, 2014 Seismic behavior of FRP-high-strength concrete-steel double skin tubular columns. *ASCE, J. Struct. Eng.* **140**(6): p. 04014019.
[20] Idris, Y. and T. Ozbakkaloglu, 2013 Seismic behavior of high-strength concrete-filled FRP tube columns. *ASCE, J. Compos. Constr.* **17**(6): p. 04013013.

[21] Idris, Y. and T. Ozbakkaloglu, 2016 Behavior of square fiber reinforced polymer-high-strength concrete-steel double-skin tubular columns under combined axial compression and reversed-cyclic lateral loading. *Eng. Struct.* **118**: p. 307 - 319.
[22] Lim, J.C. and T. Ozbakkaloglu, 2015 Hoop strains in FRP-confined concrete columns: experimental observations. *Mater. Struct.* **48**(9): p. 2839-2854.
[23] Chen, L. and T. Ozbakkaloglu, 2016 Corner strengthening of square and rectangular concrete-filled FRP tubes. *Eng. Struct.* **117**: p. 486 - 495.
[24] Ozbakkaloglu, T., 2015 A novel FRP-dual-grade concrete-steel composite column system. *Thin-Walled Structures*. **96**: p. 295-306.
[25] Vincent, T. and T. Ozbakkaloglu, 2017 Lateral strain-to-axial strain model for concrete-filled FRP tube columns incorporating interface gap and prestressed confinement. *ASCE, J. Compos. Constr.* **21**(5): p. 04017021.
[26] Lim, J.C. and T. Ozbakkaloglu, 2016 Influence of Size and Slenderness on Compressive Strain Softening of Confined and Unconfined Concrete. *Journal of Materials in Civil Engineering, ASCE*. **28**(2): p. 06015010.
[27] Ozbakkaloglu, T., A. Gholampour, and J.C. Lim, 2016 Damage-Plasticity Model for FRP-Confined Normal- and High-Strength Concrete. *Journal of Composites for Construction, ASCE*. **20**(6): p. 04016053.
[28] Lim, J.C. and T. Ozbakkaloglu, 2015 Lateral strain-to-axial strain relationship of confined concrete. *ASCE, J. Struct. Eng.* **141**(5): p. 04014141.
[29] Mansouri, I., et al., 2016 Predicting Behavior of FRP-Confined Concrete using Neuro Fuzzy, Neural Network, Multivariate Adaptive Regression Splines and M5 Model Tree Techniques. *Materials and Structures*: p. DOI:10.1617/s11527-015-0790-4.
[30] Lim, J.C. and T. Ozbakkaloglu, 2014 Unified Stress-strain model for FRP and actively confined normal-strength and high-strength concrete. *ASCE, J. Compos. Constr.* **19**(4): p. 04014072.
[31] Vincent, T. and T. Ozbakkaloglu, 2013 Influence of concrete strength and confinement method on axial compressive behavior of FRP-confined high- and ultra high-strength concrete. *Compos. Part B.* **50**: p. 413-428.
[32] Vincent, T. and T. Ozbakkaloglu, 2015 Compressive behavior of prestressed high-strength concrete-filled aramid FRP tube columns: Experimental observations. *ASCE, J. Compos. Constr.* **19**(6): p. 04015003.